Structural Characteristics for Biological Activity of Heat-Stable Enterotoxin Produced by Enterotoxigenic *Escherichia coli*: X-ray Crystallography of Weakly Toxic and Nontoxic Analogs[†,‡]

Takashi Sato, Hiroshi Ozaki, Yasuo Hata,[§] Yasuyuki Kitagawa, Yukiteru Katsube, and Yasutsugu Shimonishi*

Institute for Protein Research, Osaka University, Yamadaoka 3-2, Suita, Osaka 565, Japan

Received January 27, 1994; Revised Manuscript Received April 20, 1994[⊗]

ABSTRACT: Heat-stable enterotoxin (ST) produced by a pathogenic strain of *Escherichia coli* exerts its function by binding to a membrane-bound guanylyl cyclase on intestinal epithelial cell membranes, which in turn catalyzes the production of cyclic GMP as a second messenger in the cells. To elucidate the structural requirements for the biological activities of ST, we synthesized [Mpr[5],Gly[13]]STp(5–17) and [Mpr[5],Leu[13]]STp(5–17), which are weakly toxic and nontoxic analogs of STp, in which the toxic domain consists of the sequence from Cys at position 5 to Cys at position 17. In these analogs, Cys at position 5 is replaced by Mpr (β-mercaptopropionic acid) and Ala at position 13 by Gly and Leu, respectively. We examined these analogs by X-ray diffraction analysis using direct methods and refined the structures to crystallographic R factors of 7.3% and 6.6% using 5492 and 5122 data, respectively, observed $>3\sigma(F_o)$ with a resolution of 0.89 Å. These peptides have a right-handed spiral structure consisting of three structural segments: an N-terminal 3_{10} helix, a central type I β-turn, and a C-terminal type II β-turn. These structures show minor differences from that of [Mpr[5]]STp(5–17), the fully toxic analog of heat-stable enterotoxin [Ozaki et al. (1991) *J. Biol. Chem. 266*, 5934–5941], suggesting that the decrease and loss of the biological activities of [Mpr[5],Gly[13]]STp(5–17) and [Mpr[5],Leu[13]]STp(5–17), respectively, are not caused by structural changes but are associated with the direct interaction of Ala[13] with the receptor protein. Careful comparison of these structures in crystalline states revealed that ST has the following structural characteristics: (i) inherent flexibility at the junctions of the three segments and in the central segment, which includes the putative receptor-binding residue, Ala[13], (ii) a specific hydrophobic character around the central segment, and (iii) an unexpected C-terminal folding similar to those of functionally unrelated peptides that are known to be ionophores.

Heat-stable enterotoxins (ST)[1] are small peptides (Figure 1) that are produced by enteric bacteria such as enterotoxigenic *Escherichia coli* (Aimoto et al., 1982; Takao et al., 1983; Thompson & Giannella, 1985) and cause acute diarrheal symptoms in humans and domestic animals, which are responsible for most reported diarrheal diseases in developing countries (Smith & Gyles, 1970; Giannella, 1981). ST binds to its receptor protein on the intestinal epithelial cell membrane and activates a membrane-bound guanylyl cyclase, and the subsequent increase of cGMP concentration results in the secretion of fluid from the cells into the intestinal lumen. Previous studies on the structure–activity relationship of ST have demonstrated that the fully biologically active domain consists of the sequence from Cys at position 5 to Cys at position 17 in STp, a heat-stable enterotoxin produced by a porcine strain of enterotoxigenic *E. coli*, as shown in Figure 1 (Yoshimura et al., 1985), and have identified several potential residues involved in fluid secretion in test animals (Kubota et al., 1989; Yamasaki et al., 1990; Carpick & Gariepy, 1991; Takeda et al., 1991). Recently, the gene encoding a membrane-bound guanylyl cyclase, which has both an extracellular ST-binding domain and an intracellular cyclase catalytic domain, was cloned, and the predicted amino acid sequence of the protein was reported (Schulz et al., 1990). However, it is not known how the extracellular ligand-binding domain of the membrane-bound guanylyl cyclase recognizes the ST molecule. To answer this question, it is important to determine not only the structure of the binding site on the ST molecule but also the function of each region or residue of the ST molecule.

We recently determined the molecular structure of the toxic domain of STp by X-ray crystallography, finding that the peptide molecule consists of three segments with a 3_{10} helix, type I β-turn, and type II β-turn in order from the N-terminus, which are stabilized by three intramolecular disulfide linkages, and that the molecule as a whole is folded in a right-handed spiral (Ozaki et al., 1991). The replacement of amino acid residues by other amino acid residues in the type I β-turn segment located in the central region of STp resulted in marked reduction of the biological activity, implying that the central

[†] This work was supported in part by a Grant-in-Aid from the Ministry of Education, Science and Culture of Japan and a grant from the Yamada Science Foundation.

[‡] X-ray coordinates including hydrogen atoms, anisotropic thermal parameters, observed and calculated structure factors and other geometrical tables of [Mpr[5],Gly[13]]STp(5–17) and [Mpr[5],Leu[13]]STp(5–17) have been deposited in the Brookhaven Protein Data Bank under the file names 1ETL and 1ETM.

* Address correspondence to this author at Institute for Protein Research, Osaka University, Yamadaoka 3-2, Suita, Osaka 565, Japan. Telephone: +81-6-877-5111. Fax: +81-6-876-2533.

[§] Present address: The Institute for Chemical Research, Kyoto University, Gokasho, Uji, Kyoto 611, Japan.

[⊗] Abstract published in *Advance ACS Abstracts,* June 1, 1994.

[1] Abbreviations: ST, heat-stable enterotoxin; STp, heat-stable enterotoxin produced by a porcine strain of enterotoxigenic *Escherichia coli*; STp(5–17), synthetic analog of STp with the sequence from Cys at position 5 to Cys at position 17; Mpr, β-mercaptopropionic acid; Abu, 2-aminobutyric acid; [Mpr[5]]STp(5–17), a synthetic analog of STp(5–17) with Mpr at position 5; [Mpr[5],Gly[13]]STp(5–17) and [Mpr[5],Leu[13]]-STp(5–17), A13G and A13L in the text, synthetic analogs of [Mpr[5]]-STp(5–17) with Gly and Leu instead of Ala at position 13, respectively; rms, root mean square.

0006-2960/94/0433-8641$04.50/0

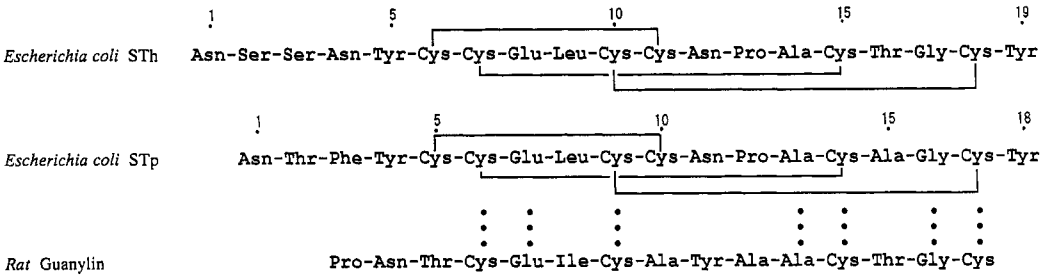

FIGURE 1: Amino acid sequences of heat-stable enterotoxins produced by enterotoxigenic *E. coli*: STh (Aimoto et al., 1982), STp (Takao et al., 1983; Thompson & Giannella, 1985), and guanylin (Currie et al., 1992).

β-turn is important for the interaction of the toxin molecule with its receptor protein (Yamasaki et al., 1990). Thus, structural analysis of analogs in which the central β-turn segment of STp is replaced is of great interest for identification of the structural motif of ST for its binding to its receptor protein, and in particular the ST-binding domain of the receptor protein. The structural and chemical features conserved for the interaction of ST with its binding protein may provide insights into this biological process. In addition, ST is a useful peptide for investigating the mechanism of recognition of a ligand by its binding protein at a molecular level, because it is a small compact molecule that is stabilized by three intramolecular disulfide linkages, as shown in Figure 1. Moreover, its structural features could be of help in molecular design of pharmaceutical useful materials such as agonists and antagonists, etc.

As one step in elucidating the structural characteristics necessary for the biological activities of the ST molecule, we report here the three-dimensional structures of crystals of A13G and A13L, which are analogs of the toxic domain of the ST molecule but with weak and no toxicity due to replacement of the Ala residue at position 13 by a Gly and Leu residue, respectively. We also demonstrate the flexibility of the molecular structure of ST for its interaction with its receptor protein and the structural features of the constituents of the ST molecule.

EXPERIMENTAL PROCEDURES

A13G and A13L were synthesized by a solid-phase procedure, purified by reversed-phase high-performance liquid chromatography, and crystallized from aqueous acetonitrile solution by gradually cooling the solution with a linear gradient temperature, as described in our previous paper (Sato et al., 1992).

The procedure for X-ray diffraction analysis was briefly as follows: single crystals shown in Table 1 were mounted and sealed in glass capillaries with a small amount of the mother liquor. Intensity data were collected at 12 °C on a Rigaku C5 automated four-circle diffractometer. Ni-filtered radiation ($\lambda = 1.54178$ Å) was produced by a Rigaku RU-300 rotating anode X-ray generator operated at 40 kV and 300 mA. The θ–2θ scan technique was used for data collection with a scan width of $(1.0 + 0.15 \tan \theta)°$, a scan rate of 2–4°/min, and $2\theta_{max} = 120°$. The background was counted for 3–4 s at both ends of each diffraction peak. The intensities of three standard reflections were measured in every 150 reflections to monitor a crystal slippage and an intensity decay due to X-ray damage. About 4000 data points were collected from each crystal, before the intensity of any standard reflection was reduced by more than 10%. Lorentz and polarization corrections, an empirical absorption correction (North et al., 1968), and a correction for X-ray damage were applied to the data. Two sets of data collected with four crystals were merged into a single set of 5097 and 6046 independent reflections at 0.89 Å for A13G and A13L, respectively. Analytical data on the crystals are summarized in Table 1.

The structures were solved by direct methods using the SHELXS86 computer program (Sheldrick, 1986) and difference Fourier techniques and refined further as described previously (Ozaki et al., 1991). Thirteen and 10 water molecules were found in the electron density maps of A13G and A13L, respectively. The water molecules were all involved in the refinement at full occupancy, which was judged by the peak heights of the atoms on Fourier maps. The numbers of water molecules were in reasonable agreement with those estimated from the differences between observed and calculated densities. All the non-hydrogen atoms were refined with anisotropic thermal parameters. The hydrogen atoms of the peptides were included in the final few cycles of refinement with isotropic thermal parameters. The isotropic equivalents of anisotropic thermal parameters of attached atoms were assigned to hydrogen atoms as initial values. The initial positions of the hydrogen atoms were calculated geometrically, although the atoms of following groups were found in difference Fourier maps: the methyl groups of Leu^8 and Ala^{15}, the side chain carboxyl group in Glu^7, and the side chain amide group of Asn^{11} in A13G; the methyl groups of Leu^8, Leu^{13}, and Ala^{15}, the side chain and C-terminal carboxyl groups of Glu^7 and Cys^{17}, and the side chain amide group of Asn^{11} in A13L. The final agreement factors were $R = 0.073$ and $R_w = 0.080$ for 5492 reflections for A13G and $R = 0.065$ and $R_w = 0.087$ for 5122 reflections for A13L with $F_o > 3\sigma(F_o)$. Unit weights were employed for A13G, and the equation $w = 1.0/[\sigma(F_o)^2 + 0.0837(F_o) + 0.0017(F_o)^2]$ was used for A13L. No residual electron density peak was observed in the final difference maps above 0.35 e/Å^3 or below –0.20 e/Å^3 for either peptide.

The atomic coordinates of the crystal structure of the [Phe^4,-Val^6]antamanide/Na^+ complex (reference code PVANSB) were retrieved from Cambridge Structural Database (Allen et al., 1991).

Computations were carried out with an NEC ACOS S930 computer in the Research Center for Protein Engineering of the Institute for Protein Research, Osaka University.

RESULTS

Molecular Structures. The molecular structures of A13G and A13L were computer-generated on the basis of the atomic coordinates obtained experimentally and are depicted in Figures 2 and 3. The observed bond lengths, bond angles, and torsion angles are within the ranges usually observed in peptides (Benedetti, 1977). These peptides consist of three structural segments which are also seen in [Mpr^5]STp(5–17), that is, a 3_{10}-helix from Mpr^5 to Cys^9, a type I β-turn from Asn^{11} to Cys^{14}, and a type II β-turn from Cys^{14} to Cys^{17} (Ozaki et al., 1991). These segments constitute the N-terminal segment from Mpr^5 to Cys^{10} and the central and the C-terminal

Table 1: Crystal Parameters

	[Mpr^5,Gly^{13}]STp(5–17)	[Mpr^5,Leu^{13}]STp(5–17)	[Mpr^5]STp(5–17)
empirical formula	$C_{45}H_{67}N_{13}O_{17}S_6 \cdot 13H_2O$	$C_{49}H_{75}N_{13}O_{17}S_6 \cdot 10H_2O$	$C_{46}H_{69}N_{13}O_{17}S_6 \cdot 13H_2O$
formula weight	1488.8	1490.8	1502.8
space group	$P2_1$	$P2_12_12_1$	$P2_12_12_1$
Z	2	4	4
crystal dimensions (mm)	0.30 × 0.36 × 0.70	0.14 × 0.33 × 0.73	0.16 × 0.23 × 0.86
	0.33 × 0.42 × 0.79	0.16 × 0.32 × 0.70	0.16 × 0.25 × 0.88
	0.34 × 0.40 × 0.88	0.16 × 0.33 × 0.74	
	0.35 × 0.40 × 0.82	0.20 × 0.38 × 0.72	
cell dimensions			
a (Å)	21.928(3)	17.892(3)	21.010(2)
b (Å)	10.219(1)	33.032(3)	27.621(4)
c (Å)	17.891(2)	12.451(1)	12.781(1)
β (deg)	111.71(1)		
V (Å^3)	3724.7	7358.6	7417.0
density			
D_{calc} (gcm^{-3})	1.327	1.346	1.346
D_{obs} (gcm^{-3})	1.350(10)	1.347(9)	1.358(1)
data resolution (Å)	0.89	0.89	0.89
total observation	12577	12749	15335
unique reflection	5907	6046	6246
unique reflection > $3\sigma(F_o)$	5492	5122	4461
weighting scheme	unit	$1/[\sigma(F_o)^2 + 0.0837(F_o) + 0.0017(F_o)^2]$	$1/[\sigma(F_o)^2 + 0.0080(F_o)^2]$
R_{merge}[a] (%)	3.3	2.5	2.4
R[b] (%)	7.3	6.5	8.9
R_w[c] (%)	8.0	8.7	9.0

[a] $R_{merge} = \sum\sum|I(i,h) - \langle I(h)\rangle|/\sum\sum I(i,h)$, where $I(i,h)$ is the intensity observed in the ith crystal and $\langle I(h)\rangle$ is the mean intensity of the reflection h for all measurements. [b] $R = \sum||F_o| - |F_c||/\sum|F_o|$. [c] $R_w = \{\sum w(|F_o| - |F_c|)^2/\sum w|F_o|^2\}^{1/2}$.

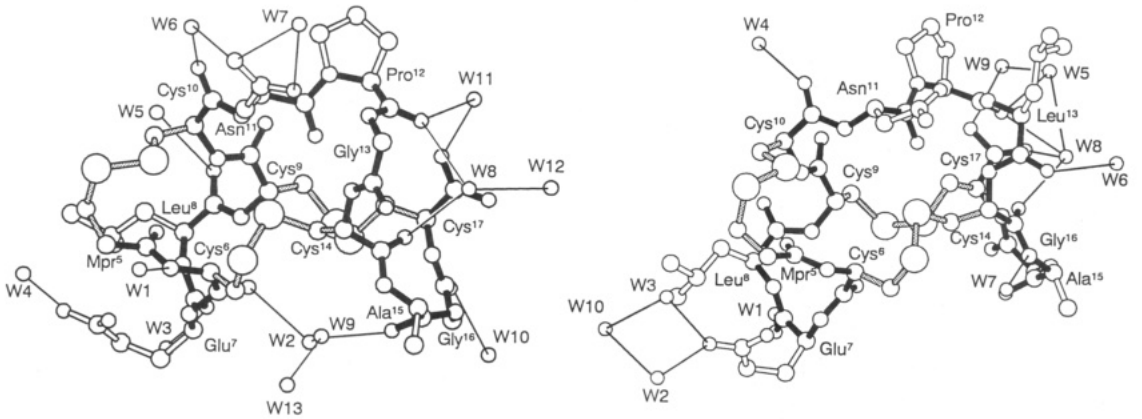

FIGURE 2: Perspective views of the refined structures of A13G (a, left) and A13L (b, right), drawn by computer using coordinates obtained experimentally. W1–W13 and W1–W10 in panels a and b, respectively, indicate the positions of oxygen atoms of water molecules. Thin lines denote hydrogen bonds between the peptides and water molecules according to the following criteria: O–O distance < 3.0 Å and an angle ∠C=O···O = 120° ± 20°; N–O distance < 3.0 Å and an angle ∠N–H···O = 180° ± 20°; between water molecules: O–O distance < 2.8 Å.

segments, respectively. Moreover, the intramolecular hydrogen bonding systems are the same as those of [Mpr^5]STp-(5–17), seem to be common to this peptide molecule, and probably play a role in keeping the molecular conformation stable. The exception is at the hydrogen bond between the hydrogen atom of the NH and the O$^{\epsilon 1}$ of Glu^7, which was not observed in the crystal structure of [Mpr^5]STp(5–17). The formation of this hydrogen bond is apparently due to the crystal packing of these molecules because the conformation of the side chain of Glu^7 is not affected by that of the toxin molecule itself. It is particularly interesting that the hydrogen bond between the CO oxygen of Mpr^5 and the NH hydrogen of Cys^{10} functions in cooperation with the disulfide bond between Mpr^5 and Cys^{10} for fixation of the conformation of the N-terminal region. The NH hydrogen atom of Cys^{10} shares its hydrogen bond acceptor, that is, the CO oxygen of Mpr^5, with the NH hydrogen of Leu^8 in good geometry. Namely, the CO oxygen of Mpr^5 is an intramolecular bifurcated hydrogen bond acceptor which has occasionally been found in other oligopeptides (Shoham et al., 1984; Taylor et al., 1984). The side chains of A13G and A13L show conformations similar to those of [Mpr^5]STp(5–17) except for Glu^7.

Geometry of Disulfide Linkages. The torsion angles (Table 2) and bond lengths of the three disulfide linkages in A13G and A13L are in good accordance with those observed previously in [Mpr^5]STp(5–17) (Ozaki et al., 1991) except for the χ'_2 values, which deviate from that in [Mpr^5]STp-(5–17). The reason for the deviation remains to be elucidated but may be due to the hinge bending motion of the central segment of the molecule, as discussed below. The characteristics of the disulfide bond geometry are that the disulfide bond between Mpr^5 and Cys^{10} has a right-hand conformation in all the analogs, and the χ_1 and χ'_1 angles are close to +60°. This conformation is quite rare, since it produces unfavorable bumps between one of two Sγ atoms of the disulfide linkage and the main chain with the exception of a few specific combinations of χ_2 values and backbone conformations (Richardson, 1981). The other two disulfide linkages between Cys^6 and Cys^{14} and Cys^9 and Cys^{17} adopt a left-handed spiral conformation, which is the most common and preferable conformation in proteins (Richardson, 1981).

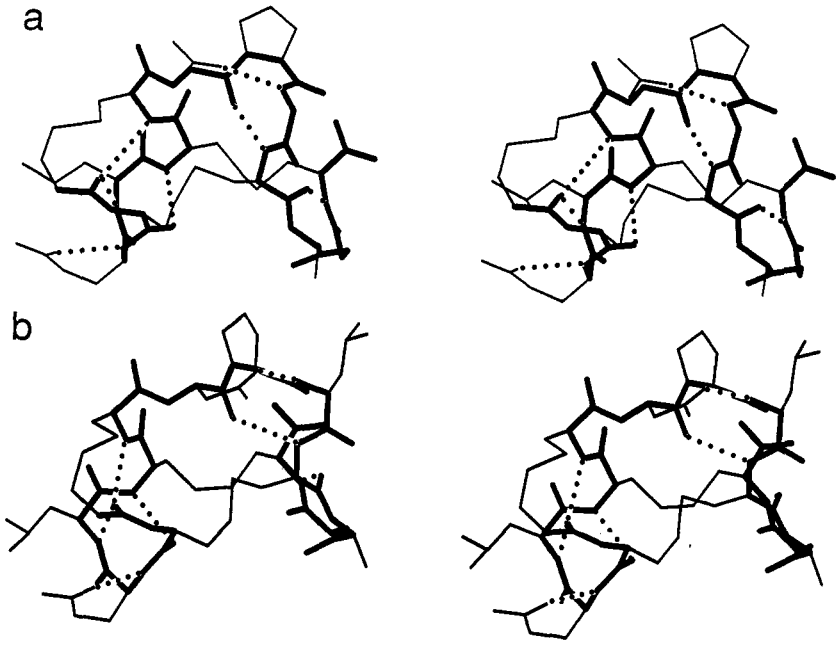

FIGURE 3: Stereodiagrams of the molecules of A13G (a) and A13L (b) viewed from the same direction as those in Figure 2. The main chains, the side chains and the disulfide bonds, and the intramolecular hydrogen bonds are delineated by thick, thin, and dotted lines, respectively.

Table 2: Torsion Angles of Disulfide Linkages of [Mpr^5,Gly^{13}]STp(5–17) (Upper), [Mpr^5,Leu^{13}]STp(5–17) (Middle), and [Mpr^5]STp(5–17) (Lower)

	torsion angles (deg)					
residue *i*	χ_1	χ_2	χ_3	χ'_2	χ'_1	residue *j*
Mpr^5	39.8[a]	61.0	78.8	178.6	69.4	Cys^{10}
	31.6[a]	65.9	78.6	−170.2	71.6	
	45.3[a]	65.7	72.5	−174.2	67.9	
Cys^6	−69.8	−60.3	−77.2	−81.6	−69.9	Cys^{14}
	−70.0	−51.2	−73.5	−95.7	−68.3	
	−80.7	−45.0	−68.2	−79.9	−64.5	
Cys^9	−70.2	−52.7	−78.6	−93.7	−60.4	Cys^{17}
	−71.9	−59.0	−80.3	−77.9	−59.1	
	−74.8	−52.7	−77.1	−76.4	−57.9	

[a] Values are calculated from the torsion angle $\theta(C,C_\alpha,C_\beta,S_\gamma)$.

Crystal Packing and Hydration. Despite to the remarkable similarities of the molecular structures of A13G and A13L to that of [Mpr^5]STp(5–17), it is evident that the former two peptides show both similarities and dissimilarities in crystal packings and hydrations to that of the latter peptide. Figure 4 shows the crystal packings of A13G and A13L with that of [Mpr^5]STp(5–17) (Ozaki et al., 1991). The crystal of A13G has a different space group of $P2_1$ from that of [Mpr^5]STp-(5–17). A13L shows the same space group of $P2_12_12_1$ as [Mpr^5]STp(5–17) but has a shorter *a*-axis and a longer *b*-axis than those of [Mpr^5]STp(5–17) (Table 1). Additionally, the arrangements of these three peptides in their crystal lattices are completely different. The most significant difference is found in the intermolecular interactions around the central segments of these three analogs. In the crystal of [Mpr^5]-STp(5–17), the central segment faces the same part of the adjacent molecule [yellow tubes of the upper and lower right molecules (C and B) in panel b of Figure 4]. However, there is little contact between these two molecules, because these segments jut out into the void space in the crystal where a bulk of water molecules exist (Ozaki et al., 1991). The crystal of A13L is more densely packed than that of [Mpr^5]STp-(5–17), and the central segment of the molecule [the yellow tube of the bottom molecule (A) in panel c of Figure 4] is tightly stacked with the N-terminal region of the screw axis related molecule [the red tube of the molecule (B)] and the translation related molecule [the bottom right molecule (A′) not shown in Figure 4] through a hydrophobic interaction. In A13G, the central segments of the two molecules face each other as in [Mpr^5]STp(5–17) [yellow tubes of molecules (A) and (B′) in panel a of Figure 4] but interact with each other more tightly than in [Mpr^5]STp(5–17). The central segment of the molecule also contacts with the N-terminal segments of the screw axis related molecule [the red tube in molecule (B′)] and translation related molecule [the red tube in molecule (A′)]. Thus, the crystal packing of A13G seems to be a hybrid between those of [Mpr^5]STp(5–17) and A13L.

In contrast to the dissimilarities of the packing arrangements, good similarities are observed in the hydration of the three ST analogs. The scheme of hydration in which water molecules bind to peptide molecules is shown in Figures 2 and 4. The specific features of the hydration that are observed in A13G and A13L are as follows: (1) Almost all the water molecules that hydrate the peptide molecules are located in the cleft region formed between the N-terminal and the C-terminal segments, around the cavity of the C-terminal segment, and around Glu^7 in the N-terminal segment. In contrast, no hydration is observed on the molecular surface around the front side of the boundaries of the three segments, which is constituted with the side chains of Cys^6, Cys^{10}, Asn^{11}, and Ala^{13}, as shown in the boundaries of the three segments (red, yellow, and blue) in the space-filling models in Figure 4. This shows that these peptides have a hydrophobic core in their central regions. The distribution of the water molecules on these ST peptides indicates that the two ST analogs, A13G and A13L, have an amphipathic character, as reported for [Mpr^5]STp(5–17) (Ozaki et al., 1991). (2) The oxygen atom of one water molecule, which corresponds to W8 in Figure 2, panels a and b, is hydrogen-bonded to the CO oxygen atoms of Pro^{12} and Cys^{14} in the crystal structures of these peptides. The geometry of this water molecule in the C-terminal region is similar in A13G and A13L and also in [Mpr^5]STp(5–17) [W6 in Figure 4 of Ozaki et al. (1991)] and is conserved much more highly than those of the other water molecules. Interestingly, two CO oxygen atoms form a pseudo-equilateral triangle with the oxygen atom of the CO group of Cys^{17}, and

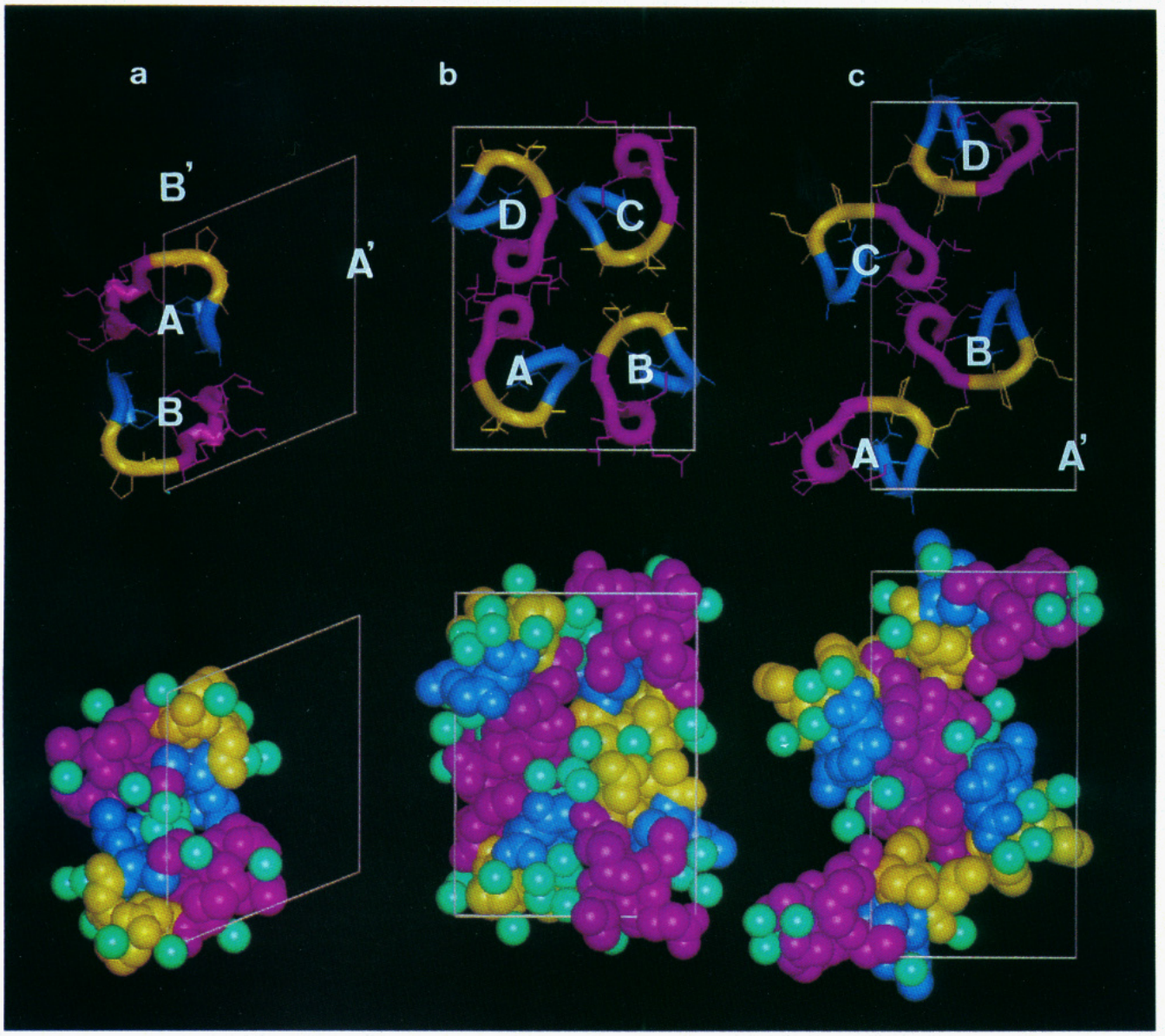

FIGURE 4: Packing diagram of the STp analogs in their crystal lattices: (a) A13G viewed down the *b*-axis, (b) [Mpr^5]STp(5–17) viewed down the *c*-axis (depicted for comparison with a and c), and (c) A13L viewed down the *c*-axis. Two different expressions are depicted to show arrangements in which the main chains and the side chains are drawn by schematic solid tubes and thin wires (upper panels) and stackings and hydrations in which all atoms are drawn by the van der Waals radii (lower panels). The N-terminal, the central, and the C-terminal segments are shown in red, yellow, and blue, respectively. The unit cells are outlined by white lines. Oxygen atoms of water molecules are indicated by green spheres.

the oxygen atom of the water molecule lies at a vertex of a tetrahedron which is formed by this water molecule and three CO oxygen atoms of the peptide molecule. Since the carboxyl oxygens of Cys^{17} are located at the C-terminus of the peptide and this carboxyl group is less restricted in its rotation, the positions of the oxygen atoms of Cys^{17} are slightly different in the three peptides. Nevertheless, this hydration polyhedron seems to be a tetrahedron with a right angle in which the oxygen atom of the water molecule occupies a corner of the right angle. This tetrahedron corresponds approximately to one part of a six-liganded octahedral coordination to a metal ion, and the position of the water molecule corresponds to that of a metal ion, as reported, for example, in a complex of (Pro-Gly)$_3$ and Ca^{2+} (Kartha et al., 1982), as discussed below.

DISCUSSION

We proposed previously that Cys-Asn-Pro-Ala-Cys at positions 10–14 of STp is a putative binding region to the receptor protein, because this sequence is conserved in all ST family members (Ozaki et al., 1991). Moreover, a part of this amino acid sequence, Ala-Cys, has recently been reported to be present in guanylin, a mammalian intestinal analog of ST, and heat-stable enterotoxin 1 isolated from enteroaggregative *E. coli* (Currie et al., 1992; Savarino et al., 1993). The replacement of the Ala residue at position 13 in STp by other amino acid residues strongly affected the toxic activities of the peptide (Yamasaki et al., 1990). These results strongly imply that this amino acid residue has a key role in the interaction of ST with its receptor protein. In this work we determined the three-dimensional structures of the weakly toxic and nontoxic analogs of STp, A13G and A13L, respectively, in which the Ala residue at position 13 in STp is replaced by Gly and Leu, respectively (Sato et al., 1992), and compared their structures with that of [Mpr^5]STp(5–17), the fully toxic analog of STp.

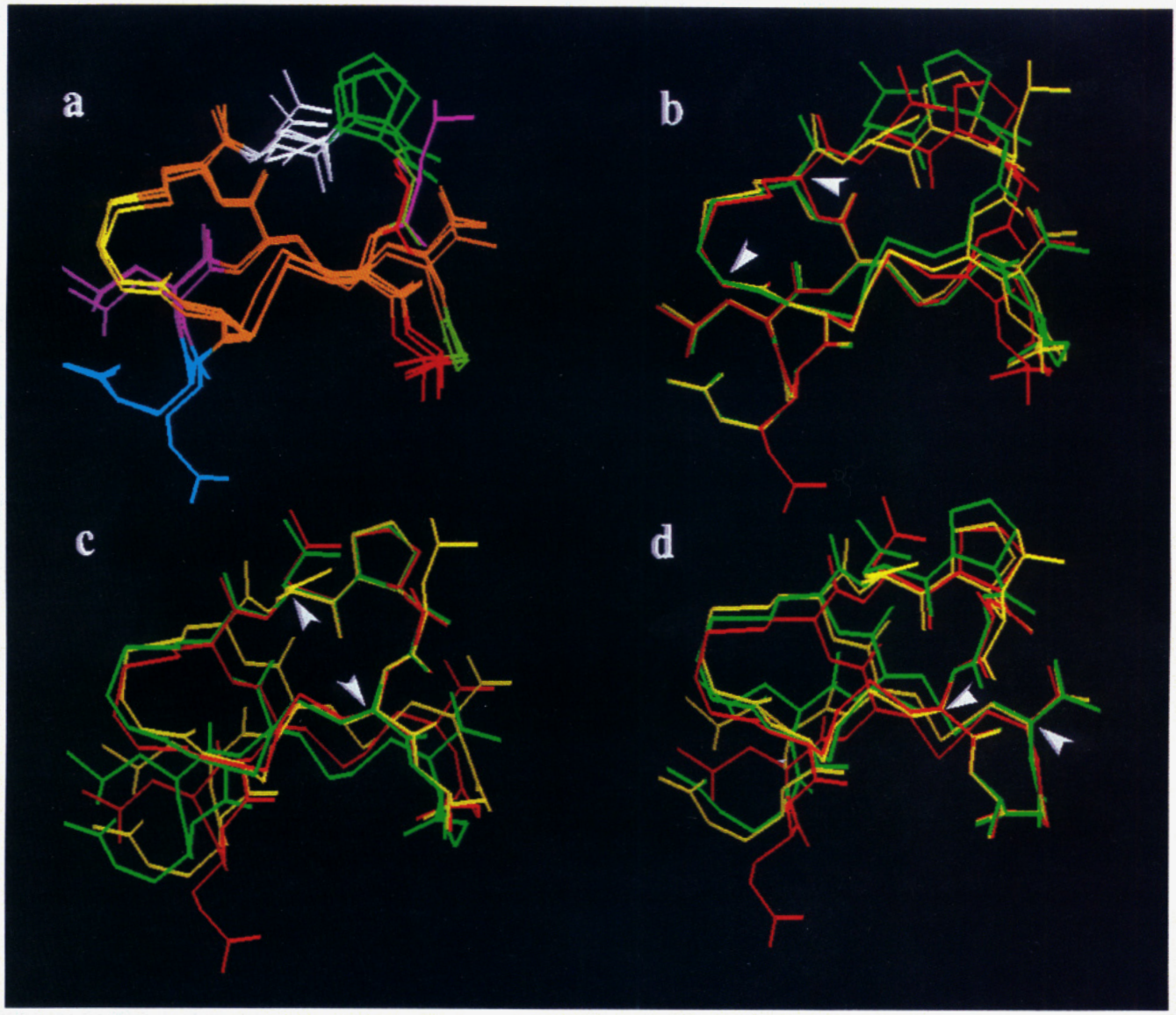

FIGURE 5: (a) Superposition of all the main-chain atoms of the structures of [Mpr^5]STp(5–17), A13G, and A13L (Mpr, yellow; Cys, orange; Glu, blue; Leu, pink; Asn, white; Pro, green; Ala, red; Gly, light green). (b – d) Superposition of the main-chain atoms in the N-terminal segment, the central segment, and the C-terminal segment [A13G (green), A13L (yellow), and [Mpr^5]STp(5–17) (red)]. Rms deviations are summarized in Table 3. Gray arrowheads indicate the Cα atoms of the terminal residues of the segments fitted and also the hinge regions (see text).

Comparison of the Structures of Toxic, Weakly Toxic, and Nontoxic STp Analogs. Figure 5a shows superpositions of the molecules of A13G and A13L on that of [Mpr^5]STp-(5–17) without hydrogen atoms. The former two molecules exhibit only small deviations from the latter molecule (see Table 3), indicating that the molecular structures of A13G and A13L do not differ substantially from that of the toxic analog, [Mpr^5]STp(5–17), although they differ slightly in detail.

Figure 6a depicts plots of the distances between the Cα atoms of A13G and A13L and those of [Mpr^5]STp(5–17) determined by superpositions of these three molecules as shown in Figure 5a. The distances are less at the five Cys residues at positions 6, 9, 10, 14, and 17 than at the other amino acid residues. This finding reveals that the relative coordinates of these five Cys residues are almost identical in these three STp peptides and also suggests that the relative orientations of these three segments in the whole molecule are different in these three peptides, because these five Cys residues reside at the junctions between these three segments and the other amino acid residues are located in these segments.

To confirm this structural characteristics of the STp molecule, we superimposed the N-terminal segment from Mpr^5 to Cys^{10}, the central segment from Asn^{11} to Cys^{14}, and the C-terminal segment from Cys^{14} to Cys^{17}, of each of the three STp molecules by least-squares calculations, as depicted in Figure 5, panels b, c, and d, respectively. The rms deviation in these superpositions are summarized in Table 3 and show that the three segments fit quite well to each other in three analogs and also fit more closely to each other than their overall structures. The result supports the proposition that these structural differences are due to variations in the relative orientations of these three segments in STp peptides, as described above. These features are also well demonstrated by a least-squares fitting in the local five residues of A13G and A13L in comparison with that of [Mpr^5]STp(5–17), as shown in Figure 6b. The largest difference between A13G and [Mpr^5]STp(5–17) is found around Cys^{14}, which is located at the junction of the central segment with the C-terminal segment, and a large difference around Cys^{10}, which connects the N-terminal segment to the central segment. On the other hand, A13L has disparity at Cys^{10}, Asn^{11}, and Pro^{12} from

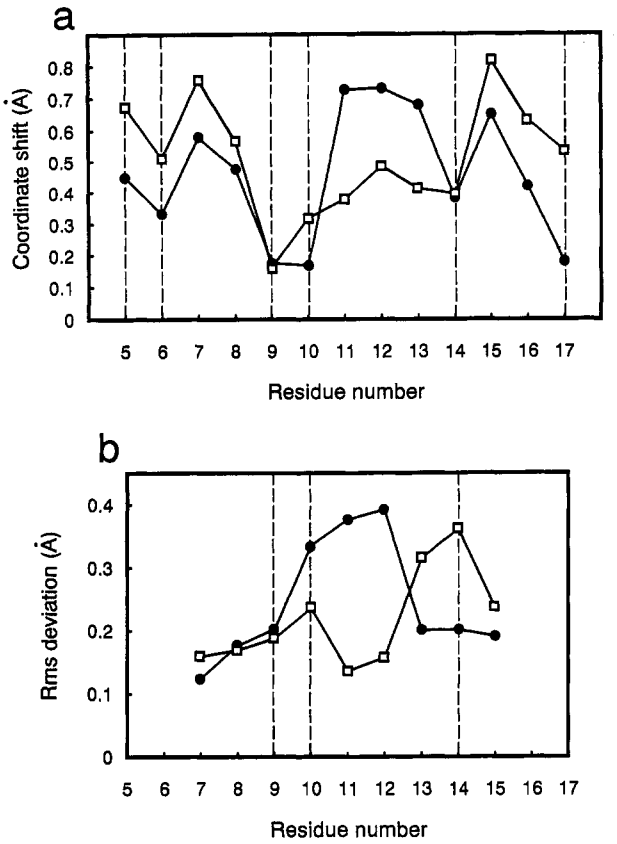

FIGURE 6: Differences between the structures of [Mpr^5]STp(5–17) and A13G (open squares) or A13L (filled circles). (Panel a) Shift plot of the distances between the Cα atoms of [Mpr^5]STp(5–17) and those of A13G or A13L based on their refined coordinates. Prior to the comparison, the respective structures were superimposed so as to minimize the rms deviation between the backbone atoms. The positions of Mpr and five Cys residues are indicated by broken lines. The shifts of these residues are smaller than those of other residues. (Panel b) Rms deviations calculated by fitting the main-chain atoms of five local residues along the amino acid sequences of the STp analogs. The central region from residue 11 to 14 of A13G and A13L deviates most from that of [Mpr^5]STp(5–17), whereas deviation of the N-terminal region is very small.

[Mpr^5]STp(5–17). Interestingly, the N-terminal segment is remarkably well fitted in both A13G and A13L to that of [Mpr^5]STp(5–17).

Rigidity and Flexibility of the STp Molecule. The conformations in the N-terminal segments of A13G and A13L seem to be more influenced by crystal packing forces than that of [Mpr^5]STp(5–17), although the main-chain differences in this region are very small. The reason for this is that the side chains of Glu^7 of both A13G and A13L fold back toward their main-chain atoms taking a sterically unfavorable conformation of the side chain (g^-g^+ in χ_1 and χ_2) which is rarely observed in proteins, whereas the side chain of Glu^7 of [Mpr^5]STp(5–17) is extended to the outside of the molecule with a g^+g^+ conformation, which is commonly observed in proteins (Janin & Wodak, 1978). This observation indicates that the main-chain conformation of the N-terminal segment is retained in spite of the difference of the effect of the crystal packing forces. In the crystal of A13L, two neighboring molecules correlated with the 2-fold screw axis along the *a*-axis have close contact in the N-terminal region of one molecule and the central region of the other molecule (Figure 4), whereas the central region of [Mpr^5]STp(5–17) is in the cluster of water molecules without any interference with neighboring molecules. Interestingly, the conformation of A13L is apparently distorted in its central segment but scarcely distorted in the N-terminal segment from that of [Mpr^5]STp(5–17), as discussed above. These results demonstrate the rigidity of the N-terminal segment and the flexibility of the central segment of the ST molecule. They are reasonably interpreted in terms of the configuration of the disulfide linkages.

The disulfide bridge between Mpr^5 and Cys^{10} joins both ends of the N-terminal segment as described above, resulting in stiffening of the N-terminal segment (Figures 2 and 3). The other two disulfide bridges, Cys^6–Cys^{14} and Cys^9–Cys^{17}, which connect both ends of the C-terminal segment to the N-terminal segment, are thought to fix the conformation of the C-terminal segment, since Cys^{14} and Cys^{17} serve as the *i* and *i*+3 residues of the C-terminal type II β-turn. The central segment is less strained by disulfide bridges than the other two segments, because this region comprises the longest interval of amino acid residues between two Cys residues in the ST molecule. This idea is also supported by the Ramachandran steric map of the three analogs, suggesting that Asn^{11} and Cys^{14}, which connect the central region to the N- and C-terminal regions, respectively, are less strained in the rotation of the main-chain torsional angle than the other residues (Ramachandran & Sasisekharan, 1968; data not shown). The conformation of this region may be stabilized in part by the hydrogen bond between the side chain CO oxygen of Asn^{11} and the main-chain NH hydrogen of the amino acid at position 13 (Ozaki et al., 1991).

Possible Role of the C-Terminal Region in the STp Molecule. Interesting findings in analyses of the molecular structures of STp analogs were that the main-chain folding in the C-terminal region is strikingly similar to those of functionally unrelated peptides such as peptidyl ionophores, and that one water molecule is located in the same position in this region in the three STp analogs. The C-terminal region of the ST molecule, from Pro^{12} to Cys^{17}, has a chipped-bowl-like conformation, as shown in Figure 7, and the three carbonyl groups of Pro^{12}, Cys^{14}, and Cys^{17} are located on the edge of this bowl spaced equally apart from each other and directed to the center of the ring built of this edge. Unexpectedly, the dimension of this structure and the spatial arrangement of these three carbonyl groups in the STp molecule are very similar to those of peptides known to be ionophores which bind a metal ion with their 3 (or 4, 6, or 8) carbonyls or hydroxyls or amides; for example, ionophore/metal ion complexes such as cyclo(Pro-Gly)$_3$/Ca^{2+} (Kartha et al., 1982) and [Phe^4,Val^6]-antamanide/Na^+ (Karle, 1974).

Figure 7 shows the superposition by a least-squares calculation of the molecular structure of [Mpr^5]STp(5–17) on that of the [Phe^4,Val^6]-antamanide/Na^+ complex so that the three carbonyl groups of Pro^{12}, Cys^{14}, and Cys^{17} of [Mpr^5]-STp(5–17) are fitted with those of Pro^8, Val^6, and Val^1, respectively, of [Phe^4,Val^6]antamanide. The spatial arrangements and directions of these carbonyl groups and the dimensions of the peptide chains are the same in these two peptides, although the backbone conformations of the two are slightly different. Interestingly, the amide NH group of Cys^{17} of [Mpr^5]STp(5–17) is also closely fitted to the carbonyl group of Pro^3 of [Phe^4,Val^6]antamanide, suggesting that the C-terminal region of the STp molecule provides a [Phe^4,Val^6]-antamanide-like ligand field, although the ST molecule seems to form a somewhat larger space than that in the antamanide peptide. The specificity of the ST molecule for metal ions is unknown, but possibly the C-terminal region binds a metal ion such as Na^+, K^+, or Ca^{2+} judging from the similarities of the spatial positioning and orientation of the three carbonyl

Table 3: Atomic rms Deviations between Two of Three Analogs

structure	fitted to	rms deviation (Å) (residue number)			
		5–10	11–14	14–17	5–17
[Mpr^5,Gly^{13}]STp(5–17)	[Mpr^5]STp(5–17)	0.159	0.114	0.162	0.532
[Mpr^5,Leu^{13}]STp(5–17)	[Mpr^5]STp(5–17)	0.145	0.196	0.104	0.460
[Mpr^5,Gly^{13}]STp(5–17)	[Mpr^5,Leu^{13}]STp(5–17)	0.141	0.139	0.134	0.380

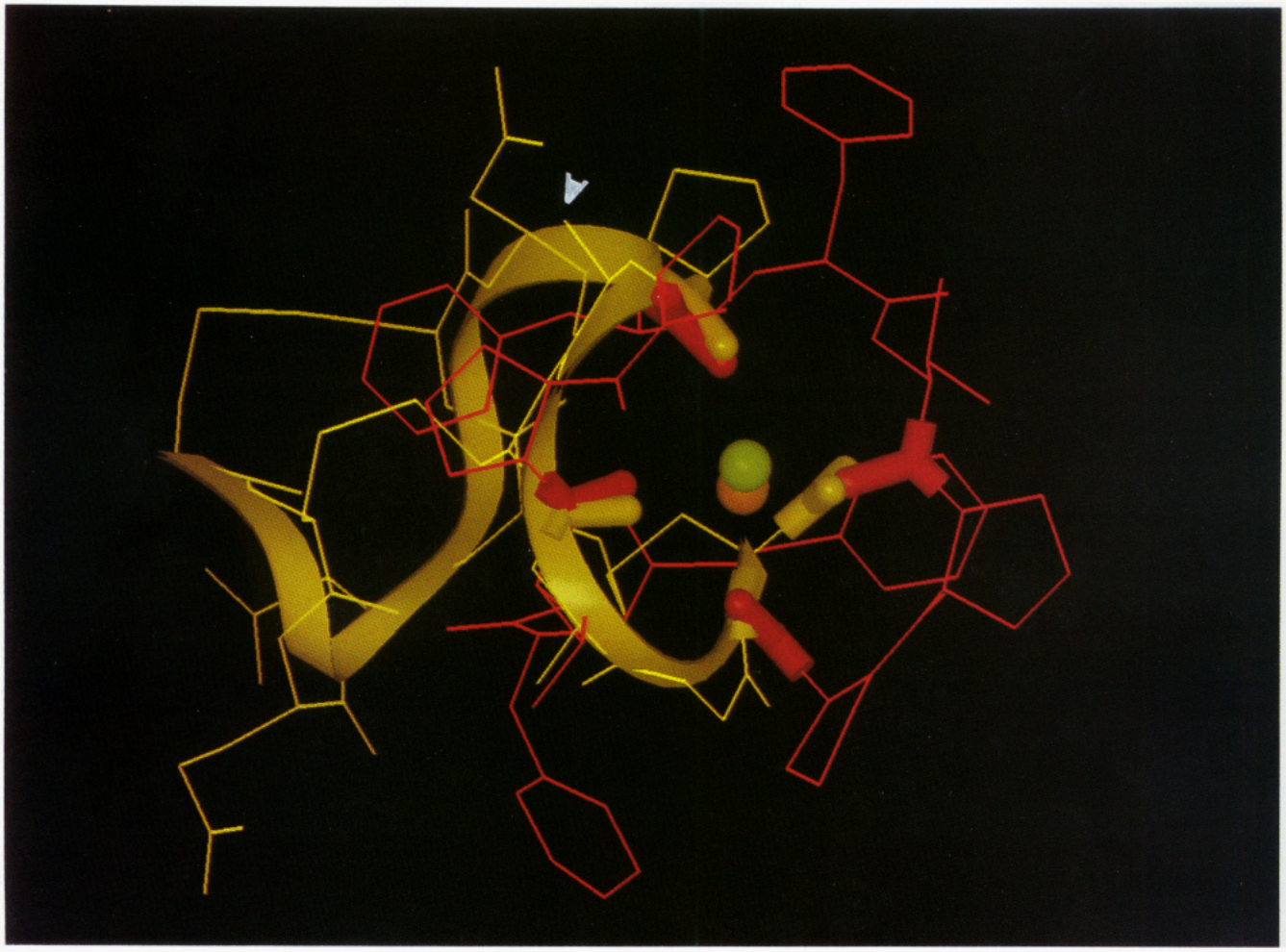

FIGURE 7: Comparison of the structures of [Mpr^5]STp(5–17) (pale yellow) and an ionophore, the [Phe^4,Val^6]antamanide/Na$^+$ complex (red line) (Karle, 1974). The two peptides are fitted so as to minimize the distances between their corresponding carbonyl groups (see text). These carbonyls and the NH nitrogen atom of Cys^{17} in [Mpr^5]STp(5–17) are shown by rods. Na$^+$ ion complexed to the antamanide and oxygen atom of specific hydrated water in the STp molecule are indicated by orange and green spheres, respectively (see text). The main-chain flow of [Mpr^5]STp(5–17) is indicated by a yellow ribbon, and the methyl group of Ala^{13} of [Mpr^5]STp(5–17) is shown by a gray arrowhead.

groups of Pro^{12}, Cys^{14}, and Cys^{17} and the conformation of the C-terminal region to those of ionophore peptides. These considerations suggest that ST may function as a cation-binding peptide.

Previous studies provided evidence that ST exerts a Ca^{2+} ionophore-like function; for example, the fluid secretion from the intestine involving the activation of a Ca^{2+}-dependent regulator protein caused by increase of the passive Ca^{2+} uptake by Ca^{2+} ionophores such as A23187 (Iludain & Naftalin, 1979), the dose-dependent stimulation of Ca^{2+} uptake by the addition of ST to rat basophilic leukemia cell cultures (Knoop & Thomas, 1983), and the quantitative relationship between electrolyte secretion and Ca^{2+} channel-blocker insensitive Ca^{2+} influxes induced by ST (Goyal et al., 1987). Thus, an important role of the C-terminal region for the biological activity of ST may be a cation binding function as an ionophore, because the structural characteristics of this region closely resemble those of typical peptidyl ionophores as shown above. However, the relation between the signal transduction pathway mediated by the receptor protein, a membrane-bound guanylyl cyclase, and the fluid secretion stimulated by Ca^{2+} is not well understood, and it is unknown how ST acts as an ionophore.

Naturally occurring mutants of STp which have Phe or Thr at position 15 in the C-terminal region are active, suggesting that the activity of ST is unaffected by amino acid substitutions at this position. Moreover, replacement of Gly^{16} by Ala has no effect on the enterotoxigenic activity (Carpick & Gariepy, 1991). These results indicate that side chain substitution in the C-terminal segment does not affect the toxic activity of ST. On the other hand, the C-terminal region is essential for the toxic activity of ST, because the decapeptide [Ala^{10}]STp(5–14) in which the C-terminal segment of the peptide is lost has greatly decreased activity (Yamasaki et al., 1988; Carpick & Gariepy, 1991). These conflicting observations suggest that the main chain in the C-terminal segment is important for the toxicity of ST.

Structure–Function Relationships of STp. We previously reported that the replacement by amino acid residues with

larger side chains, such as Abu and Leu, of Ala at position 13 in STp, which lies in the central segment of the toxin, resulted in marked decrease or complete loss in the enterotoxicity, whereas the substitution of Ala^{13} by amino acid residues with a rather small side chain such as Gly or Ser in [Mpr^5]STp(5–17) resulted in only moderate reduction (about 3-fold decrease) in the enterotoxicity (Yamasaki et al., 1990; Sato et al., 1992). The decrease in the enterotoxicity of STp by these substitutions has been ascribed to decrease in binding affinity to the receptor protein (Yamasaki et al., 1990; Carpick & Gariepy, 1991). The substitution of Asn^{11} in STp by a charged amino acid residue such as Asp, Glu, Arg, or Lys causes about 100–1000-fold decrease in the toxic activity (Okamoto et al., 1988; Takeda et al., 1991), whereas its replacement by Val does not affect the activity (Takeda et al., 1991). Removal of the side chain of Pro^{12} (replacement by Gly) causes considerable decrease in both the binding affinity and the enterotoxicity (Waldman et al., 1989), but other substitutions at this residue result in only moderate reduction of the toxicity; for instance, replacement of Pro^{12} by Val or Ala causes only 3- or 4-fold decrease in the enterotoxicity (Carpick & Gariepy, 1991; Takeda et al., 1991).

These data suggest that there is a hydrophobic pocket on the receptor surface which comes into a close contact with the side chain of Ala^{13} in STp and that the toxin molecule binds to the receptor protein mainly through hydrophobic interaction. This interaction is well supported by both the present finding that the central region of ST forms an hydrophobic core and the fact that a bile salt is able to dissociate the ST–receptor complex without great loss of the binding ability of the receptor protein (Hugues et al., 1992).

The present study demonstrated that the conformations of A13G and A13L, which are weakly toxic and nontoxic analogs, respectively, are virtually identical to that of [Mpr^5]STp(5–17), the fully toxic analog, and that the slight differences of the conformations in the central segments of these analogs are caused by crystal packing forces to the inherently flexible part of the ST molecule. These findings indicate that the loss of the enterotoxicity by replacing Ala^{13} by Leu is simply attributable to increase of the bulkiness of the side chain (length, capacity) which prevents specific interaction with the receptor protein. On the contrary, the decrease of the enterotoxicity by replacing Ala^{13} by Gly is considered to be due mainly to loss of the methyl group, which reduces the interaction of ST with the receptor protein through the methyl group of Ala^{13}. Consequently, we conclude that the difference in potencies of these analogs is caused only by the structures of their side chains at position 13, and that the receptor protein specifically recognizes the defined structure around Ala^{13} of ST. However, the critical loss of the enterotoxicity resulted from replacement of the methyl group of Ala by the larger side chain of an amino acid residue such as Abu suggests that another region around the methyl group is also important for the ST–receptor interaction.

Figure 8 depicts the space-filling model of [Mpr^5]STp(5–17), showing the bulk arrangement of the atoms around Ala^{13}. The methyl group of Ala^{13} juts out to the upper-left top of the plane of the paper from the upper-right corner of the model. Other residues or atoms that interact with the receptor protein have to be located around the methyl group of Ala^{13} in a three-dimensional sense. Candidate atoms in this context are the Sγ of Cys^{10}, the atoms of Asn^{11} and Pro^{12}, and the C_β of Ala^{15}, because they share the surface in a direction similar to that of the methyl group of Ala^{13}. The atoms in Cys^{14}, which is the neighbor of Ala^{13}, are not included among these

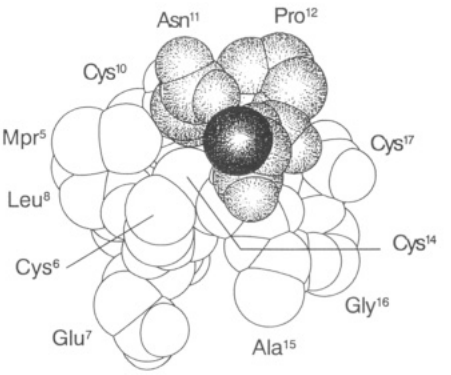

FIGURE 8: Space-filling model of [Mpr^5]STp(5–17) without hydrogen atoms depicting the bulk arrangement of the atoms around Ala^{13}, which is strongly suggested to be part of the binding interface. The methyl carbon atom of Ala^{13} and the atoms of Asn^{11}, Pro^{12}, and Ala^{13} are shaded heavily and lightly, respectively. These atoms form the main portion of the hydrophobic core of the ST molecule, judging from the manner of hydration in the crystals (see the text).

candidates, because the side chain atoms and the main chain amide group of Cys^{14} are directed into the interior of the molecule and are hidden from other residues too completely to contact with a binding region on the surface of the receptor protein. Indeed, Cys^{14} is the only residue in the toxin molecule that has no solvent-accessible surface, as shown by calculation of the accessible surface area (data not shown). Thus, because of the unique conformation of the molecule, the side chain and the main chain of Cys^{14} cannot interact with the receptor protein, although the disulfide bridge between Cys^6 and Cys^{14} is important for maintaining the conformation of the toxin molecule and therefore for expression of the toxic activity (Gariepy et al., 1987; Yamasaki et al., 1988). The side chain methyl group of Ala^{15}, which is arranged in the same direction as that of Ala^{13}, is also not a candidate, because naturally occurring mutants at this position have the same toxicity as that of STp (Aimoto et al., 1982; Takao et al., 1985). The receptor binding region of the toxin estimated from the spatial arrangement of the atoms is mainly constituted from the side chain and main chain of Asn^{11} and Pro^{12} in addition to Ala^{13}, compatible with previous findings that Asn^{11}, Pro^{12}, and Ala^{13} are the most important residues for the activity (Takeda et al., 1991) and that the toxicity of STp is less affected by substitution of Glu^7, Leu^8, and Gly^{16}, which are located on the opposite side of Ala^{13} (Yoshimura et al., 1986; Carpick & Gariepy, 1991).

Guanylin, a mammalian analog of heat-stable enterotoxin, was recently identified to be an endogenous ligand for a membrane-bound guanylyl cyclase in rat and human small intestine (Currie et al., 1992; Wiegand et al., 1992). Guanylin has complete sequence homology to the C-terminal part of STp including the Ala^{13} residue in its central segment, while it has less homology to the N-terminal and central segments of STp and lacks the disulfide bridge in the N-terminal segment corresponding to that between Cys^5 and Cys^{10} in STp (Figure 1). This sequence homology between guanylin and STp supports the idea of the importance of Ala^{13} in ST for molecular recognition of the receptor protein and the structural and biological implication of the C-terminal segment discussed above, although the presence of the C-terminal segment itself is not sufficient for its receptor binding and biological activity (Yamasaki et al., 1988; Carpick & Gariepy, 1991). Interestingly, Asn^{11} and Pro^{12} in STp are not found at the relatively same positions in guanylin, but nevertheless they are replaced by hydrophobic residues (Tyr and Ala, respectively), which are thought to form a hydrophobic core with the conserved

Ala residue corresponding to Ala^{13} of STp.

Judging from the fact that the disulfide linkage not found in guanylin corresponds to the bridge in the N-terminal segment of ST that is important for making a rigid pillar, it is considered that the rigidity of the N-terminal segment is important for ST to maintain its enterotoxicity under the severe physiological conditions in intestinal organs of the host animal. This idea is supported by the fact that guanylin is rapidly degraded by components present in the intestinal tract of infant mice, whereas ST is strongly resistant to digestion by them (Carpick & Gariepy, 1993). On the contrary, the flexibility of the central region of ST described above is essential for ST as an exogenous ligand to fit into the binding site of the target protein, which is actually the receptor protein for a natural endogenous ligand.

In conclusion the structural characteristics of the ST molecule are summarized as follows: (i) Three segments, a 3_{10} helix from the N-terminal Mpr^5 to Cys^9, type I β-turn from Asn^{11} to Cys^{14}, and type II β-turn from Cys^{14} to the C-terminal Cys^{17}, form independent structural units in the ST molecule and share quite similar conformations in three analogs, although these three units are firmly joined by disulfide linkages, (ii) the ST molecule is flexible at the junctions between two of these three structural segments, and the conformation of the central region is changed by replacing the constituent amino acids at given positions by others, even though the change is slight and may be due to the crystal packing of the ST molecules, (iii) the conformation of the N-terminal segment is most stable and is conserved in three ST analogs, suggesting that this structure plays a role as a nucleation for formation of the spatial structure of the ST molecule, (iv) the central segment is structurally flexible and Ala^{13} is directed to the outside of the molecule, whereas Cys^{14} is completely buried inside the molecule. Thus Ala^{13} rather than Cys^{14} is implicated in the function of the ST molecule, and (v) the C-terminal region including the C-terminal type II β-turn structure confines a water molecule by coordinating to three CO oxygen atoms which are members of the β-turn structure. This C-terminal structure may play a role in binding a cation instead of a water molecule under physiological conditions and may act as an ionophore transporting a metal ion from the outside of the cells into the inside.

ACKNOWLEDGMENT

We thank Mrs. Aiko Kobatake and Miss Fukiko Nagano for preparation of the manuscript.

REFERENCES

Aimoto, S., Takao, T., Shimonishi, Y., Hara, S., Takeda, T., Takeda, Y., & Miwatani, Y. (1982) *Eur. J. Biochem. 129*, 257–263.

Allen, F. H., Davies, J. E., Galloy, J. J., Johnson, O., Kennard, O., Macrae, C. F., Mitchel, E. M., Mitchel, G. F., Smith, J. M., & Watson, D. G. (1991) *J. Chem. Inf. Comput. Sci. 31*, 187–204.

Benedetti, E. (1977) in *Peptides—Proceedings of the Fifth American Peptide Symposium* (Goodman, M., & Meienhofer, J., Eds.) pp 257–279, Wiley, New York.

Carpick, B. W., & Gariepy, J. (1991) *Biochemistry 30*, 4803–4809.

Carpick, B. W., & Gariepy, J. (1993) *Infect. Immun. 61*, 4710–4715.

Currie, M. G., Fok, K. F., Kato, J., Moore, R. J., Hamra, F. K., Duffin, K. L., & Smith, C. E. (1992) *Proc. Natl. Acad. Sci. U.S.A. 89*, 947–951.

Gariepy, J., Judo, A. K., & Schoolnik, G. K. (1987) *Proc. Natl. Acad. Sci. U.S.A. 84*, 8907–8911.

Giannella, R. A. (1981) *Annu. Rev. Med. 32*, 341–357.

Goyal, J., Ganguly, N. K., Mahajan, R. C., Garg, U. C., & Walis, N. S. (1987) *Biochim. Biophys. Acta 925*, 341–346.

Hugues, M., Crane, M. R., Thomas, B. R., Robertson, D., Gazzano, H., O'Hanley, P., & Waldman, S. A. (1992) *Biochemistry 31*, 12–16.

Iludain, A., & Naftalin, R. J. (1979) *Nature 279*, 446–448.

Janin, J., & Wodak, J. (1978) *J. Mol. Biol. 125*, 357–386.

Karle, I. L. (1974) *Biochemistry 13*, 2155–2162.

Kartha, G., Varughese, K. I., & Aimoto, S. (1982) *Proc. Natl. Acad. Sci. U.S.A. 79*, 4519–4522.

Knoop, F. C., & Thomas, D. D. (1983) *Infect. Immun. 41*, 971–977.

Kubota, H., Hidaka, Y., Ozaki, H., Ito, H., Hirayama, T., Takeda, Y., & Shimonishi, Y. (1989) *Biochem. Biophys. Res. Commun. 161*, 229–235.

North, A. C. T., Phillips, D. C., & Mathews, F. S. (1968) *Acta Crystallogr. A24*, 351–359.

Okamoto, K., Okamoto, K., Yukitake, J., & Miyama, A. (1988) *Infect. Immun. 56*, 2144–2148.

Ozaki, H., Sato, T., Kubota, H., Hata, Y., Katsube, Y., & Shimonishi, Y. (1991) *J. Biol. Chem. 266*, 5934–5941.

Ramachandran, G. N., & Sasisekharan, V. (1968) *Adv. Protein Chem. 23*, 283–438.

Richardson, J. S. (1981) *Adv. Protein Chem. 34*, 167–363.

Sato, T., Ito, H., Takeda, Y., & Shimonishi, Y. (1992) *Bull. Chem. Soc. Jpn. 65*, 938–940.

Savarino, S. J., Fasano, A., Watson, J., Martin, B. M., Levine, M. M., Guandalini, S., & Guerry, P. (1993) *Proc. Natl. Acad. Sci. U.S.A. 90*, 3093–3097.

Schulz, S., Green, C. K., Yuen, P. S. T., & Garbers, D. L. (1990) *Cell 63*, 941–948.

Sheldrick, G. M. (1986) SHELXS86, Program for Crystal Structure Solution, University of Goettingen, Federal Republic of Germany.

Shoham, G., Lipscomb, W. N., & Wieland, Th. (1984) *J. Am. Chem. Soc. 111*, 4791–4809.

Smith, H. W., & Gyles, C. L. (1970) *J. Med. Microbiol. 3*, 387–401.

Takao, T., Hitouji, T., Aimoto, S., Shimonishi, Y., Hara, S., Takeda, T., Takeda, Y., & Miwatani, T. (1983) *FEBS Lett. 152*, 1–5.

Takao, T., Shimonishi, Y., Kobayashi, M., Nishimura, O., Arita, M., Takeda, T., Honda, T., & Miwatani, T. (1985) *FEBS Lett. 193*, 250–254.

Takeda, Y., Yamasaki, S., Hirayama, T., & Shimonishi, Y. (1991) in *Molecular Pathogenesis of Gastrointestinal Infections* (Wadstrom, T., et al., Eds.) pp 125–138, Plenum Press, New York.

Taylor, R., Kennard, O., & Versichel, W. (1984) *J. Am. Chem. Soc. 106*, 244–248.

Thompson, M. R., & Giannella, R. A. (1985) *Infect. Immun. 47*, 834–836.

Waldman, S. A., & O'Hanley, P. (1989) *Infect. Immun. 57*, 2420–2424.

Wiegand, R. C., Kato, J., Huang, M. D., Fok, K. F., Kachur, J. F., & Currie, M. G. (1992) *FEBS Lett. 311*, 150–154.

Yamasaki, S., Hidaka, Y., Ito, H., Takeda, Y., & Shimonishi, Y. (1988) *Bull. Chem. Soc. Jpn. 61*, 1701–1706.

Yamasaki, S., Sato, T., Hidaka, Y., Ozaki, H., Ito, H., Hirayama, T., Takeda, Y., Sugimura, T., Tai, A., & Shimonishi, Y. (1990) *Bull. Chem. Soc. Jpn. 63*, 2063–2070.

Yoshimura, S., Ikemura, H., Watanabe, H., Aimoto, S., Shimonishi, Y., Hara, S., Takeda, T., Miwatani, T., & Takeda, Y. (1985) *FEBS Lett. 181*, 138–142.

Yoshimura, S., Takao, T., Shimonishi, Y., Hara, S., Arita, M., Takeda, T., Imaiishi, H., Honda, T., & Miwatani, T. (1986) *Biopolymers 25*, S69–S83.